



Since January 2020 Elsevier has created a COVID-19 resource centre with free information in English and Mandarin on the novel coronavirus COVID-19. The COVID-19 resource centre is hosted on Elsevier Connect, the company's public news and information website.

Elsevier hereby grants permission to make all its COVID-19-related research that is available on the COVID-19 resource centre - including this research content - immediately available in PubMed Central and other publicly funded repositories, such as the WHO COVID database with rights for unrestricted research re-use and analyses in any form or by any means with acknowledgement of the original source. These permissions are granted for free by Elsevier for as long as the COVID-19 resource centre remains active.



# Computational and experimental studies on the inhibitory mechanism of hydroxychloroquine on hERG

Ran Yu<sup>a,\*</sup>, Peng Li<sup>b</sup>

<sup>a</sup> Department of Bioengineering, Beijing Polytechnic, Daxing District, Beijing, 100176, China

<sup>b</sup> SDIC Xinkai Water Environment Investment Co., Ltd, Tongzhou District, Beijing, 101101, China

## ARTICLE INFO

Handling Editor: K. Wallace

### Keywords:

Hydroxychloroquine  
hERG  
Arrhythmia  
Molecular docking  
Patch clamp technique

## ABSTRACT

Hydroxychloroquine (HCQ) was noted to produce severe cardiac arrhythmia, an adverse effect as its use against severe acute respiratory syndrome caused by coronavirus 2 (SAES-CoV-2). HCQ is an antimalarial drug with quinoline structure. Some other quinoline compounds, such as fluoroquinolone antibiotics (FQs), also lead to arrhythmias characterized by QT prolongation. QT prolongation is usually related to the human ether-a-go-go-related gene (hERG) potassium channel inhibitory activity of most drugs. In this research, molecular docking was used to study the potential inhibitory activities of HCQ as well as other quinolines derivatives and hERG potassium channel protein. The possible causes of these QT prolongation effects were revealed. Molecular docking and patch clamp experiments showed that HCQ could bind to hERG and inhibit the efflux of potassium ion preferentially in the repolarization stage. The IC<sub>50</sub> of HCQ was 8.6 μM ± 0.8 μM. FQs, which are quinoline derivatives, could also bind to hERG molecules. The binding energies of FQs varied according to their molecular polarity. It was found that drugs with a quinoline structure, particularly with high molecular polarity, can exert a significant potential hERG inhibitory activity. The potential side effects of QT prolongation during the development and use of quinolines should be carefully considered.

## 1. Introduction

Hydroxychloroquine (HCQ) is a derivative of 4-aminoquinolone, which has a quinolone structure similar to that of fluoroquinolone antibiotics (FQs) (Bensalah, Midassi et al. 2020). HCQ has been used as an antimalarial medicine for a long time. Since the outbreak of coronavirus disease (COVID-19), HCQ has been used to fight against severe acute respiratory syndrome coronavirus 2 (SARS-CoV-2); however, this treatment has been found to lead to arrhythmic and cardiovascular side effects (Sridhar, Chatterjee et al. 2020; Voisin, Lorc'h et al. 2020). FQs are widely used broad-spectrum antibiotics (Redgrave, Sutton et al. 2014), which can also lead to serious arrhythmias, characterized by QT prolongation (Porta et al., 2019), suggesting a correlation between the quinolone structure and arrhythmia.

QT interval prolongation is dominated by the human ether-a-go-go-related gene (hERG) encoded (Vandenberg, Perry et al. 2012) voltage-gated K<sup>+</sup> channels (Robertson and Morais-Cabral, 2020). The early repolarization of cardiac AP includes a transient outward of potassium channel current (IKr) (Wu and Sanguinetti, 2016; Butler, Zhang et al. 2019), and some compounds (Gualdani, Cavalluzzi et al. 2017),

particularly many antibiotics and HCQ (Wang and MacKinnon, 2017), may restrain the K<sup>+</sup> outflow (Vaz, Kang et al. 2018; Cavalluzzi, Imbriani et al. 2020). Inhibition of the hERG channel would lead to a reduction in IKr and repolarization reserve, subsequently causing QT prolongation (Nachimuthu, Assar et al. 2012). The hERG channel in which HEK cells is expressed (Lee, Choi et al. 2019), is widely employed to evaluate the potential risk of medicines. In vitro ion patch clamp assays were used to evaluate the potential inhibition of hERG channels (Ridder, Leishman et al. 2020), and the value of the half inhibitory concentration (IC<sub>50</sub>) was adopted to indicate the degree of QT prolongation (Kongsamut, Kang et al. 2002). The patch clamp technique is a widely used technique to evaluate the inhibitory activities of compounds in ion channel models by measuring ionic currents (Lei, Clerx et al. 2019). The whole-cell patch-clamp electrophysiological technique (Rohrbacher, Damiano et al. 2015; Stoelzle-Feix, Brinkwirth et al. 2020) is the “gold standard” for ion channel analysis (Acter, Uddin et al. 2020; Gao, Zhang et al. 2020). FQs have been synthesized by the introduction of a fluorine atom in quinoline, which also increased the incidence of arrhythmia (Song, Wang et al. 2020). Different structural characteristics of FQs lead to great differences in their hERG inhibitory activities (Zünkler and Wos,

\* Corresponding author.

E-mail address: [yuran1230@hotmail.com](mailto:yuran1230@hotmail.com) (R. Yu).

<https://doi.org/10.1016/j.tox.2021.152822>

Received 14 March 2021; Received in revised form 8 May 2021; Accepted 24 May 2021

Available online 28 May 2021

0300-483X/© 2021 Elsevier B.V. All rights reserved.

2003). For example, at the same concentrations, norfloxacin and lomefloxacin inhibited hERG currents by  $2.8\% \pm 3.6\%$  and  $12.3\% \pm 4.7\%$ , respectively (Zünkler, Claaßen et al. 2006). According to the studies on the interactions between hERG and FQs, the binding sites of FQs reside in the region around the amino acid residues TYR652s, SER624, and PHE656s of the hERG channel (Ryu, Imai et al. 2013; Khondker, Bider et al. 2021). In this study, the potential inhibitory activities of quinolones including HCQ and 15 FQs (ofloxacin, gatifloxacin, norfloxacin, ciprofloxacin, orbifloxacin, difloxacin, pefloxacin, fleroxacin, enrofloxacin, lomefloxacin, sarafloxacin, enoxacin, balofloxacin, danofloxacin, and nadifloxacin) on hERG channels were evaluated by molecular docking, and the inhibitory activity of HCQ at the whole-cell level was further evaluated using patch clamp. The study of the binding activity of compounds to hERG potassium channel protein is of great significance for the evaluation cardiotoxicity and drug safety of quinolones (Dong, Liu et al. 2019; Cheng, Du et al. 2019).

## 2. Materials and methods

### 2.1. Molecular docking

The structures of the ligand compounds were drawn using ChemDraw, and all the structures were optimized using the classical MM2 force field. The cryo-EM structure of the hERG-related K<sup>+</sup> channel (Protein Data Bank [PDB] ID: 5va1) was downloaded from PDB (<http://www1.rcsb.org>) and used as the model. AutoDock Vina software was applied in all the docking experiments, and the optimized model of the hERG related K<sup>+</sup> channel was used as the docking target. During molecular docking, the macromolecular receptor hERG channel was treated as rigid. The docking site was confirmed according to the known interaction sites between FQs and the hERG channel, and the potential inhibitory activity of HCQ as well as the underlying mechanism was studied. A grid box ( $60 \text{ \AA} \times 60 \text{ \AA} \times 60 \text{ \AA}$ ) centered at (81.800, 69.459, 93.127) Å for the hERG channel was adopted in the docking experiments using the Auto Dock tools.

### 2.2. Molecular dynamics study

Based on molecular docking, the root mean square deviation (RMSD) of docking molecules was simulated and evaluated to further explain and analyze the potential hERG K<sup>+</sup> channel inhibitory activity of HCQ. To validate the structural stability and conformational flexibility of the binding complex, protein-ligand complex molecular dynamics were investigated using Discovery Studio 2020 (DS). The hERG channel protein was prepared under the DS macromolecular module, based on which protein solvation was performed using the CHARMM force field. Molecular dynamics simulation, including minimization, heating, equilibrium, and production, was performed using a standard dynamics cascade. The RMSD of conformations is in the unit of Å, and the unit of equilibrium time is picosecond (ps). The simulation time of the equilibrium phase was 20 ps, and that of the production phase was 200 ps.

### 2.3. Inhibitory activity of HCQ on hERG

#### 2.3.1. Materials

Dulbecco's modified Eagle's medium (DMEM), fetal bovine serum (FBS), and TrypLE™ Express were purchased from Gibco (China). DMSO, cisapride, Potassium aspartate, NaCl, KCl, EGTA, MgCl<sub>2</sub>•6H<sub>2</sub>O, D-Glucose, CaCl<sub>2</sub>•2H<sub>2</sub>O, and Na<sub>2</sub>-ATP were purchased from Sigma-Aldrich (China).

#### 2.3.2. Cell culture

The HEK-293 cell line of the hERG potassium channel was purchased from Creacell Company (product number: a-0320). Cells were maintained in DMEM supplemented with 10% (v/v) fetal bovine serum FBS (0.8 mg/mL) at 37 °C and 5% (v/v) CO<sub>2</sub>. The hERG currents were

elicited by whole-cell technique in the voltage-clamp mode. The peak tail current density was used to assess the voltage dependence of the activation or inactivation of compounds (Shugg, Somberg et al. 2020). The elicited tail current density in the cells was applied to draw a current-voltage plot.

#### 2.3.3. Cell passage

The old medium was removed, and the cells were washed once with phosphate-buffered saline. TrypLE™ express solution (1 mL) was added and the solution was incubated at 37 °C for 0.5 min. When the cells detached from the dish bottom, approximately 5 mL of complete medium preheated at 37 °C was added. Subsequently, the cell suspension was gently blown with a pipette to separate the aggregated cells. The cells were centrifuged at 1000 rpm for 5 min. After amplification or maintenance culture, the cells were inoculated in a culture dish, at a density of  $2.5 \times 10^5$  cells.

#### 2.3.4. Patch clamp

The external solution was comprised of 140 mM NaCl, 3.5 mM KCl, 1 mM MgCl<sub>2</sub>•6H<sub>2</sub>O, 2 mM CaCl<sub>2</sub>•2H<sub>2</sub>O, 10 mM D-glucose, 10 mM HEPES buffer, and 1.25 mM NaH<sub>2</sub>PO<sub>4</sub>•2H<sub>2</sub>O, and the pH was adjusted to 7.4. The internal solution contained 20 mM KCl, 115 mM Potassium aspartate, 1 mM MgCl<sub>2</sub>•6H<sub>2</sub>O, 5 mM EGTA, 10 mM HEPES buffer, and 2 mM Na<sub>2</sub>-ATP, and the pH of internal solution was 7.2.

Whole-cell recordings were obtained as follows: when the whole-cell mode was established, the clamp voltage was fixed at  $-80$  mV. The clamp voltage changed to  $-50$  mV by depolarization (holding for 0.5 s), stepped to 30 mV (holding for 2.5 s), and finally reduced to  $-50$  mV (holding for 4 s) to excite the tail current of the hERG channel. Data were collected every 10 s to observe the effect of the compounds on the tail current. A  $-50$  mV stimulation for 0.5 s was selected for the detection of the leakage current. The data were processed using patchmaster (Heka) software.

The electrode was fabricated from borosilicate capillaries. The cell membrane was pulled by the microelectrode manipulator, and a GΩ seal was formed through negative pressure. Following this, rapid capacitance compensation was performed, and then the negative pressure was continued to be applied to break the cell membrane for the whole-cell recording. Then, slow capacitance was compensated, and the membrane capacitance and series resistance were recorded to study the correlation between compound concentration and voltage. When the current was stable, different concentrations of the compounds were detected for 5 min.

The cell was placed in a recording chamber affixed at the stage of an inverted microscope. The compounds and the external liquid without the compounds flowed through recording bath from low to high concentrations by gravity irrigation. During the recording, the liquid was exchanged with a vacuum pump. Each cell served as its own control group according to the current detected in the external liquid. Three cells were detected independently and repeatedly detected in each group. All electrophysiological tests were performed at room temperature.

Further, 30 mM storage solution was prepared. 10.08 mg of HCQ was weighed, dissolved in 1% sulfuric acid, and then diluted by ultrapure water to prepare 30 mM storage solution. Concentrations of 0.3, 1, 3, and 10 μM were prepared by dilution of the storage solution with ultrapure water, respectively. These stock dilutions of the compound were diluted in turn with extracellular solution to prepare 0.3, 1, 3, 10, and 30 μM solutions. Cisapride was used as the control. The experiments were performed in triplicate. The data deviation of the experiments was evaluated using standard deviation.

The current for each compound was first standardized. Then, the inhibition rate corresponding to each concentration was calculated according to Eq. (1).

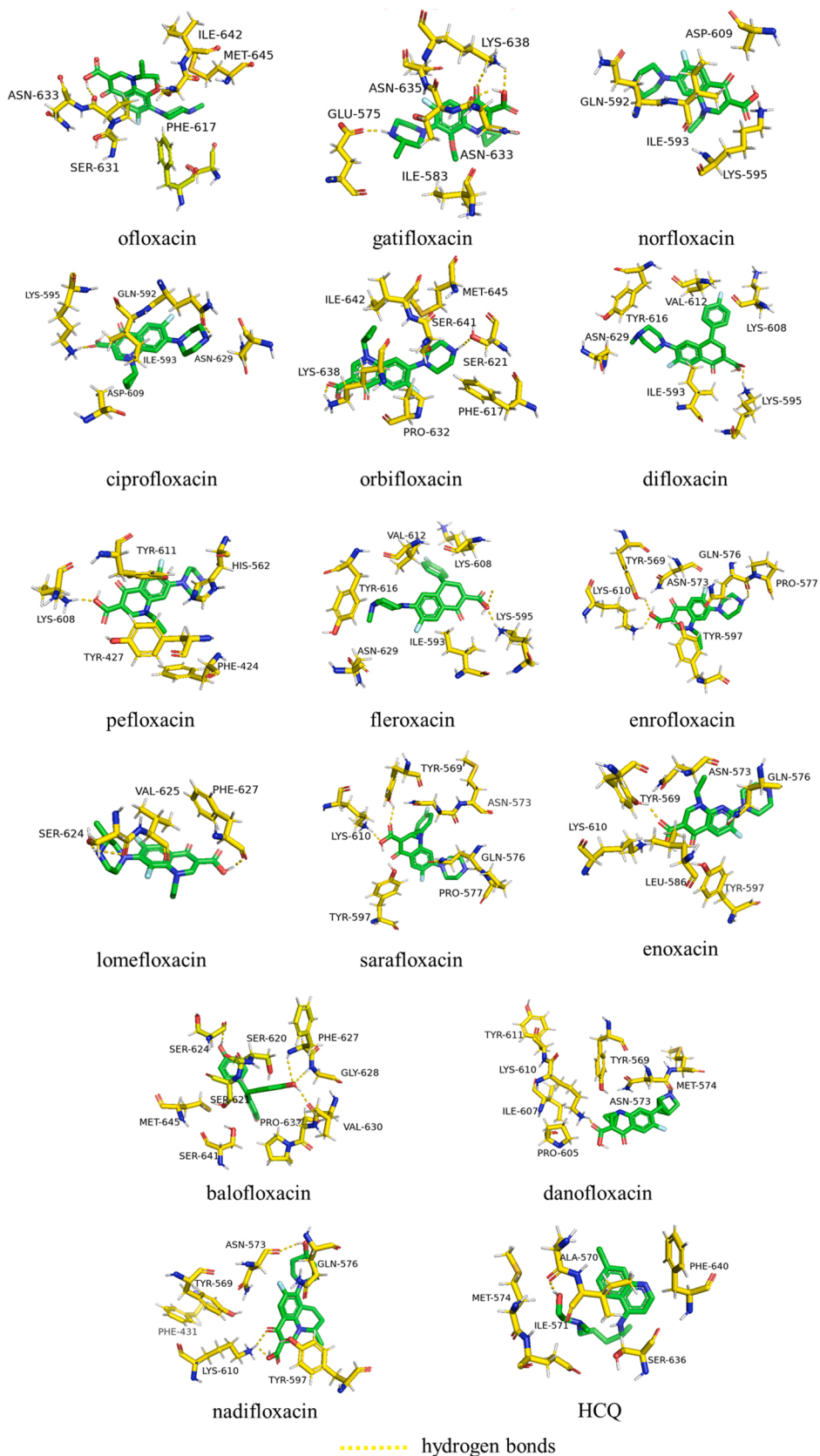


Fig. 1. Binding region of hERG.

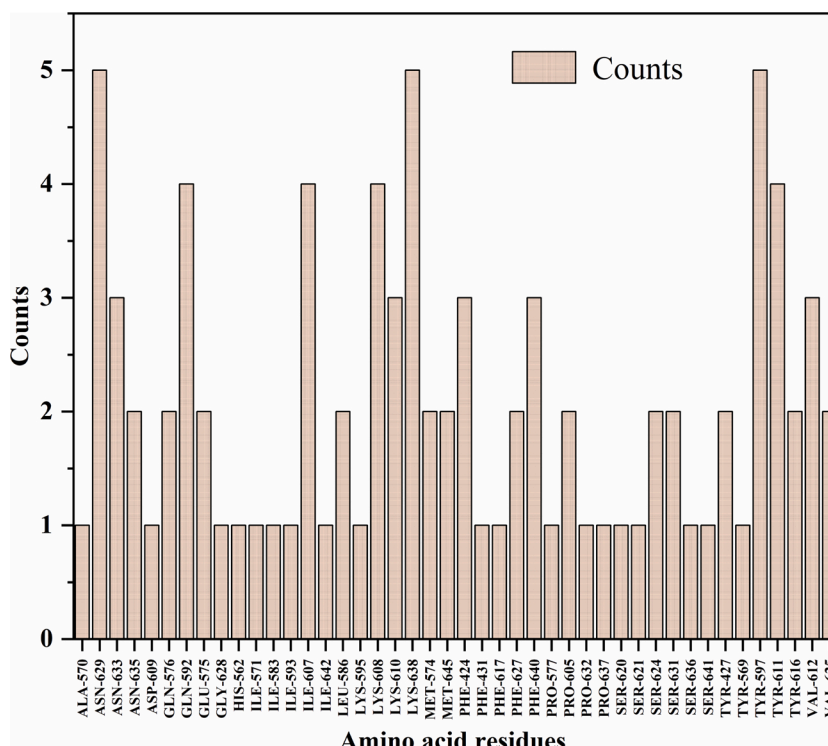


Fig. 2. Amino acid residues in binding site.

$$\text{inhibition} = 1 - \frac{\text{Peak tail current compound}}{\text{Peak tail current vehicle}}$$

$$\text{inhibition} = \frac{1}{1 + \left(\frac{IC_{50}}{C}\right)^h}$$

- (1) The Eq. (2) was used to fit the dose-dependent effect nonlinearly, where C was the concentration of the test substance, IC<sub>50</sub> was the half inhibitory concentration, and h was the Hill coefficient. Curve fitting and IC<sub>50</sub> (Lei, Clerx et al. 2019; Ridder, Leishman et al. 2020) calculations were performed using IGOR software.
- (2)

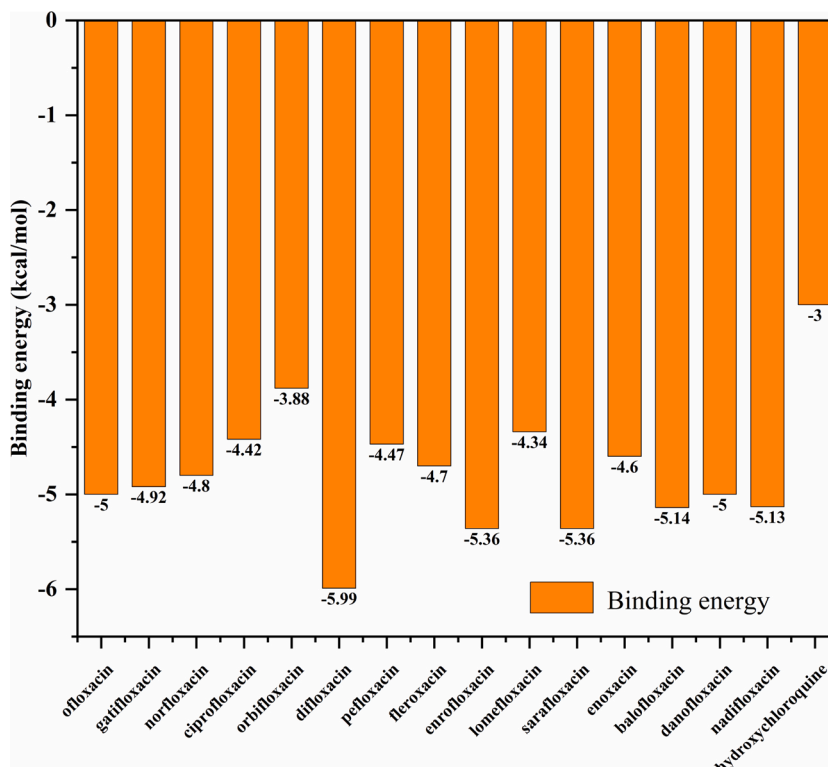


Fig. 3. Binding energy.

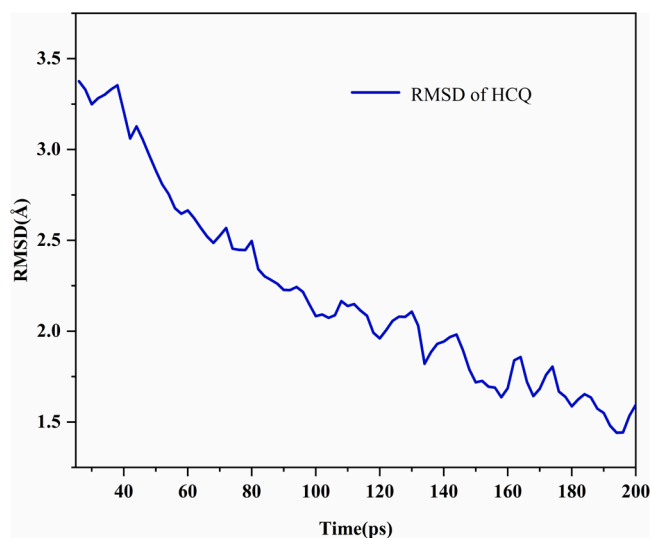


Fig. 4. RMSD of HCQ binding complex with hERG.

### 3. Results

#### 3.1. Molecular docking

Both FQs and HCQ could bind to hERG (Fig. 1). The main amino acid residues that interacted with compounds were ASN-629, GLN-592, ILE-607, LYS-608, LYS-610, LYS-638, TYR-597, TYR-611, VAL-612, PHE-424, and PHE-640 (Fig. 2).

Ofloxacin formed a hydrogen bond with ASN-633, a  $\pi$ -cation contact with PHE-617, and hydrophobic reactions with ILE-642, MET-645, and SER-631. Gatifloxacin formed 3-H bonds with LYS-638, GLU-575, and ASN633, and hydrophobic reactions with ASN-635 and ILE-583. Norfloxacin bound to channel proteins mainly through hydrophobic force. Ciprofloxacin formed 2-H bonds with LYS-595 and ASN-629, and hydrophobic reactions with GLN-592, ILE-593, and ASP-609. Orbifloxacin formed 2-H bonds with LYS-638 and SER-621, a  $\pi$ -cation contact with PHE-617, and hydrophobic forces with ILE-642, SER-641, MET-645, and PRO-632. Difloxacin formed a hydrogen bond with LYS-595, and hydrophobic forces with ASN-629, TYR-616, VAL-612, LYS-608, and ILE-593. Pefloxacin formed a hydrogen bond with LYS-608, a  $\pi$ -cation contact with PHE-424, and hydrophobic forces with TYR-611, HIS-562, and TYR-427. Fleroxacin formed a hydrogen bond with LYS-595, and hydrophobic forces with LYS-608, VAL-612, TYR-616, ASN-629, and ILE-593. Enrofloxacin formed 3-H bonds with LYS-610, PRO-577, and TYR-569, a  $\pi$ -cation contact with TYR-597, and hydrophobic forces with GLN-576 and ASN-573. Lomefloxacin formed 2-H bonds with SER-624 and PHE-627, and hydrophobic force with VAL-525. Sarafloxacin formed 2-H bonds with LYS-610 and TYR-569, a  $\pi$ -cation contact with TYR-597, and hydrophobic forces with GLN-576, ASN-573, and PRO-577. Enoxacin formed a hydrogen bond with TYR-569, and hydrophobic forces with LYS-610, LEU-586, GLN-576, ASN-573, and TYR-597. Balofloxacin formed 4-H bonds with SER-624, GLY-628, PHE-627, and VAL-630, and hydrophobic forces with SER-620, SER-621, SER-641, MET-645, and PRO-632. Danofloxacin formed a hydrogen bond with LYS-610. Nadifloxacin formed 3-H bonds with LYS-610, TYR-597, and ASN-573. HCQ formed a hydrogen bond with ALA-570, a  $\pi$ -cation contact with PHE-640, and hydrophobic forces with MET-574, ILE-571, and SER-636. From the perspective of binding energy (Fig. 3), FQs bound to hERG with lower energies, which showed easier combinations.

#### 3.2. RMSD

The RMSD values of HCQ and hERG binding complex were stable at approximately 1.5 Å (Fig. 4), which illustrated that the dock was stable.

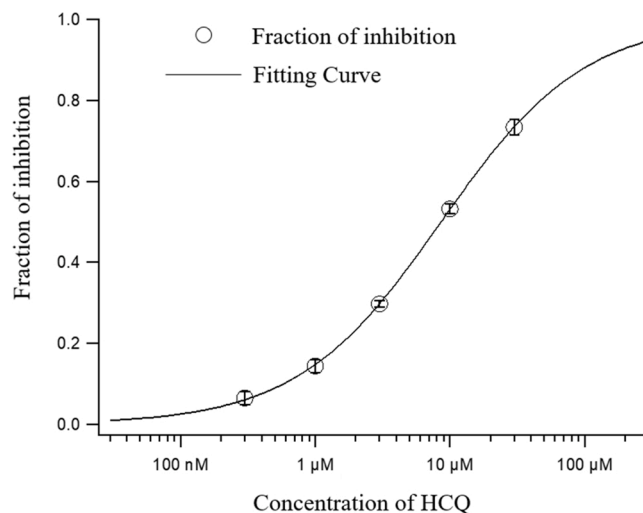


Fig. 5. hERG inhibition curve of HCQ.

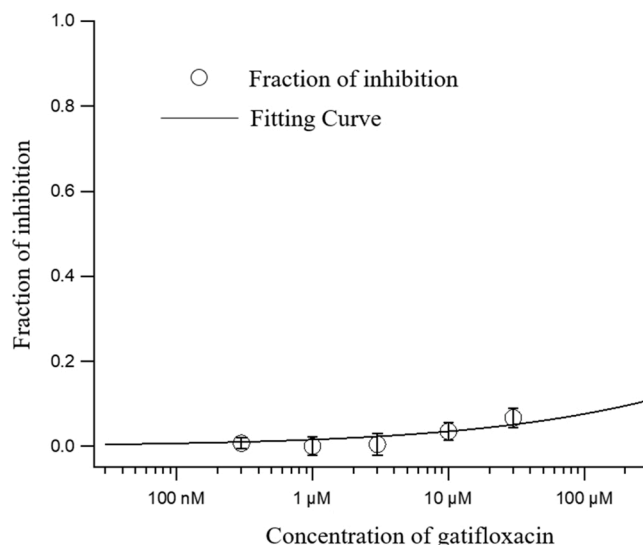


Fig. 6. hERG inhibition curve of gatifloxacin.

Amino acid residue ALA-570 formed a hydrogen bond with HCQ, and the hydrogen bond and other hydrophobic forces stabilized the structure of the complex. HCQ bound to hERG channel protein effectively, and inhibited the outflow of  $K^+$ , resulting in QT prolongation.

#### 3.3. Patch clamp

According to the results of molecular docking, the average binding energy of FQs was  $-4.9$  kcal/mol. Gatifloxacin with a binding energy of  $-4.9$  kcal/mol was chosen to represent FQs and be compared with HCQ.

HCQ showed a concentration dependent inhibition of the hERG potassium channel during the patch clamp experiments. When the concentrations of HCQ were 0.3, 1, 3, 10 and 30  $\mu\text{M}$ , the rates of inhibition ( $n = 3$ ) of the hERG channel were  $6.52\% \pm 2.74\%$ ,  $14.49\% \pm 2.73\%$ ,  $29.76\% \pm 1.37\%$ ,  $53.25\% \pm 2.07\%$ , and  $73.43\% \pm 3.17\%$ , respectively. The hERG  $\text{IC}_{50}$  value of HCQ was  $8.6\mu\text{M} \pm 0.8\mu\text{M}$  (Fig. 5). Gatifloxacin also showed concentration dependent inhibitory activity. When the concentrations were 10 and 30  $\mu\text{M}$ , the rates of inhibition ( $n = 3$ ) of the hERG channel were  $3.53\% \pm 3.57\%$  and  $6.72\% \pm 3.99\%$  (Fig. 6), respectively. The current traces of IKr in hERG-HEK cells exposure to different concentrations of HCQ (Fig. 7) and gatifloxacin (Fig. 8) were normalized.

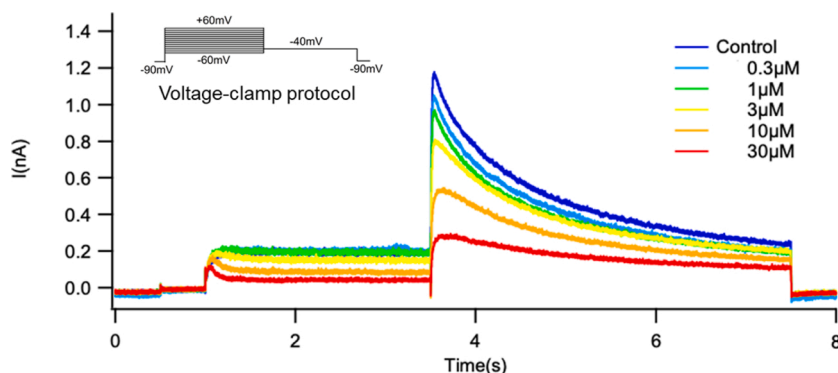


Fig. 7. Normalized current traces of IKr in hERG-HEK cells exposure to different concentrations of HCQ.

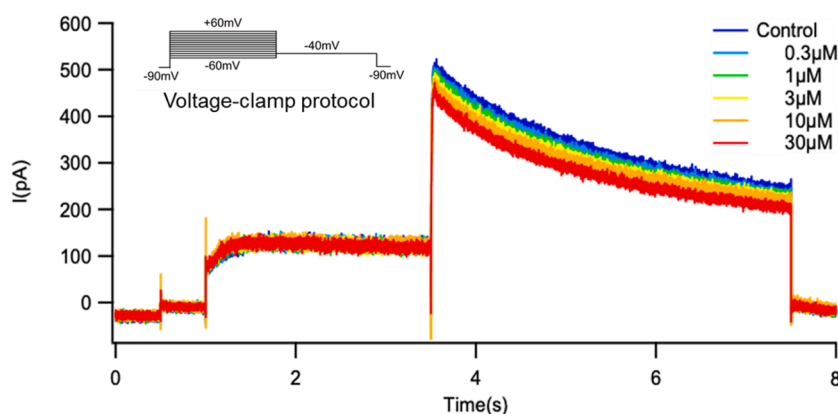


Fig. 8. Normalized current traces of IKr in hERG-HEK cells exposure to different concentrations of gatifloxacin.

#### 4. Discussion

Based on the results of amino acid analysis, lysine, which facilitates the formation of hydrogen bonds, was found to be more involved in the formation of interactions with HCQ and FQs. The structures of FQs are similar, thus the amino acid residues that interact with FQs are more concentrated, such as LYS-610 and its adjacent amino acid residues. The binding target of HCQ is remarkably close to that of the FQs. PHE-640 amino acid residue formed hydrogen bond interactions with FQs and HCQ. FQs introduce fluorine atoms into the structure, which enhances the polarity of the molecules. Compared with other FQs, difloxacin with an additional fluorine atom had the lowest binding energy, followed by enrofloxacin and sarafloxacin. The amino acid residues of the site which interacted with enrofloxacin and sarafloxacin were identical. Compared with FQs, HCQ had larger binding energy, which indicated that the introduction of functional groups such as fluorine atom with larger polarity into quinoline structure was of great significance to stabilize the interactions between compounds and receptors. Increasing the polarity of quinoline compounds might lead to stronger binding to hERG K<sup>+</sup> channel protein.

Analysis of the binding sites of HCQ and FQs indicated the structure dependent binding ability of quinoline compounds to hERG. HCQ and gatifloxacin had a concentration dependent inhibitory effect on the hERG channel. The inhibitory activity to hERG channel protein of gatifloxacin was lower than that of HCQ. The inhibitory activity of gatifloxacin illustrated that the structure of FQs was related to the inhibition of hERG, which was consistent with the results of molecular docking. During the analysis of amino acid residues involved in the binding of HCQ and gatifloxacin, two common binding regions were found, one consists of LYS-638, ASN-635, ASN-633, and PHE-640, the other consists of GLU-575 and MET-574. In addition, HCQ interacted with ALA-570 and ILE-571 amino acid residues specially, which

indicated that ALA570 and ILE-571 was the key binding region that affected the inhibitory activity of hERG. The combination of HCQ, FQs, and remdesivir may synergistically inhibit hERG channels, and disrupt repolarization reserve, since remdesivir was also reported to block K<sup>+</sup> currents (Chang, Liu et al. 2020). The electrical activity of the heart is realized by the inward and outward currents. Besides hERG, the inhibition of inwardly-rectifying potassium channels may also be responsible for the prolongation of QT interval (Akyuz and Villa, 2020).

#### 5. Conclusion

HCQ and FQs share the same quinoline structure and have similar molecular polarities. All studied compounds could dock with hERG K<sup>+</sup> channel protein to form a complex. The binding sites of HCQ and FQs are similar, however, the introduction of fluorine atoms in FQs reduced the binding energy during the docking process. The docking energies of FQs were lower than that of HCQ, and the binding energy of difloxacin was the lowest. The polarity of molecules might affect the binding energy and the stability of the complex. The main amino acid residues involved in the binding sites were ASN-629, GLN-592, ILE-607, LYS-608, LYS-610, LYS-638, TYR-597, TYR-611, VAL-612, PHE-424, and PHE-640. HCQ and FQs interacted with hERG mainly through hydrogen bond and hydrophobic forces. Molecular dynamics simulation analysis showed that a stable molecular complex was formed by the docking of HCQ and hERG. These results suggest that HCQ can inhibit K<sup>+</sup> efflux by binding to the hERG potassium channel protein, resulting in a prolonged cardiac QT interval. The hERG IC<sub>50</sub> value of HCQ was 8.6µM.

The inhibition of HCQ on the outflow of K<sup>+</sup> from the hERG potassium channel is the main cause of cardiac arrhythmia. More attention should be paid to the cardiotoxicity of quinoline compounds, especially HCQ, which has been used as a potential drug against SARS-CoV-2.

## Declaration of Competing Interest

The authors report no declarations of interest.

## Acknowledgements

Authors wish to thank general projects of scientific research plan of Beijing Municipal Commission of Education for financial support under the project KM202010858002.

## References

- Acter, T., Uddin, N., Das, J., Akhter, A., Choudhury, T.R., Kim, S., 2020. Evolution of severe acute respiratory syndrome coronavirus 2 (SARS-CoV-2) as coronavirus disease 2019 (COVID-19) pandemic: a global health emergency. *Sci. Total Environ.* 730, 138996.
- Akyuz, E., Villa, C., 2020. A novel role of cardiac inwardly rectifying potassium channels explaining autonomic cardiovascular dysfunctions in a cuprizone-induced mouse model of multiple sclerosis. *Auton. Neurosci.* 225, 102647.
- Bensalah, N., Midassi, S., Ahmad, M.I., Bedoui, A., 2020. Degradation of hydroxychloroquine by electrochemical advanced oxidation processes. *Chem. Eng. J.* 402, 126279.
- Butler, A., Zhang, Y., Stuart, A.G., Dempsey, C.E., Hancox, J.C., 2019. Functional and pharmacological characterization of an S5 domain hERG mutation associated with short QT syndrome. *Heliyon* 5 (4), e01429.
- Cavalluzzi, M.M., Imbrici, P., Gualdani, R., Stefanachi, A., Mangiatordi, G.F., Lentini, G., Nicolotti, O., 2020. Human ether-à-go-go-related potassium channel: exploring SAR to improve drug design. *Drug Discov. Today* 25 (2), 344–366.
- Chang, W.-T., Liu, P.-Y., Zi-Han, G., Lee, S.-W., Lee, W.-K., Wu, S.-N., 2020. Evidence for the effectiveness of remdesivir (GS-5734), a nucleoside-analog antiviral drug in the inhibition of I K(M) or I K(DR) and in the stimulation of I MEP. *Front. Pharmacol.* 11, 1091.
- Cheng, H., Du, C., Zhang, Y., James, A.F., Dempsey, C.E., Abdala, A.P., Hancox, J.C., 2019. Potent hERG channel inhibition by sarizotan, an investigative treatment for Rett Syndrome. *J. Mol. Cell. Cardiol.* 135, 22–30.
- Dong, X., Liu, Y., Niu, H., Wang, G., Dong, L., Zou, A., Wang, K., 2019. Electrophysiological characterization of a small molecule activator on human ether-a-go-go-related gene (hERG) potassium channel. *J. Pharmacol. Sci.* 140 (3), 284–290.
- Gao, J., Zhang, H., Xiong, P., Yan, X., Liao, C., Jiang, G., 2020. Application of electrophysiological technique in toxicological study: from manual to automated patch-clamp recording. *TrAC Trends Anal. Chem.* 133, 116082.
- Gualdani, R., Cavalluzzi, M.M., Tadini-Buoninsegni, F., Lentini, G., 2017. Discovery of a new mexiletine-derived agonist of the hERG K<sup>+</sup> channel. *Biophys. Chem.* 229, 62–67.
- Khondker, A., Bider, R.-C., Passos-Gastaldo, I., Wright, G.D., Rheinstädter, M.C., 2021. Membrane interactions of non-membrane targeting antibiotics: the case of aminoglycosides, macrolides, and fluorquinolones. *Biochim. Biophys. Acta (BBA) – Biomembr.* 1863 (1), 183448.
- Kongsamut, S., Kang, J., Chen, X.-L., Roehr, J., Rampe, D., 2002. A comparison of the receptor binding and HERG channel affinities for a series of antipsychotic drugs. *Eur. J. Pharmacol.* 450 (1), 37–41.
- Lee, H.J., Choi, B.H., Choi, J.-S., Hahn, S.J., 2019. Effects of cariprazine on hERG 1A and hERG 1A/3.1 potassium channels. *Eur. J. Pharmacol.* 854, 92–100.
- Lei, C.L., Clerx, M., Gavaghan, D.J., Polonchuk, L., Mirams, G.R., Wang, K., 2019. Rapid characterization of hERG channel kinetics I: using an automated high-throughput system. *Biophys. J.* 117 (12), 2438–2454.
- Nachimuthu, S., Assar, M.D., Schussler, J.M., 2012. Drug-induced QT interval prolongation: mechanisms and clinical management. *Ther. Adv. Drug Saf.* 3 (5), 241–253.
- Porta, L., Lee, M.-t.G., Hsu, W.-T., Hsu, T.-C., Tsai, T.-Y., Lee, C.-C., 2019. Fluoroquinolone use and serious arrhythmias: a nationwide case-crossover study. *Resuscitation* 139, 262–268.
- Redgrave, L.S., Sutton, S.B., Webber, M.A., Piddock, L.J.V., 2014. Fluoroquinolone resistance: mechanisms, impact on bacteria, and role in evolutionary success. *Trends Microbiol.* 22 (8), 438–445.
- Ridder, B.J., Leishman, D.J., Bridgland-Taylor, M., Samieegohar, M., Han, X., Wu, W.W., Randolph, A., Tran, P., Sheng, J., Danker, T., Lindqvist, A., Konrad, D., Hebeisen, S., Polonchuk, L., Gissinger, E., Renganathan, M., Koci, B., Wei, H., Fan, J., Levesque, P., Kwagh, J., Imredy, J., Zhai, J., Rogers, M., Humphries, E., Kirby, R., Stoelzle-Feix, S., Brinkwirth, N., Rotordam, M.G., Becker, N., Friis, S., Rapedius, M., Goetze, T.A., Strassmaier, T., Okeyo, G., Kramer, J., Kuryshev, Y., Wu, C., Himmel, H., Mirams, G.R., Strauss, D.G., Bardenet, R., Li, Z., 2020. A systematic strategy for estimating hERG block potency and its implications in a new cardiac safety paradigm. *Toxicol. Appl. Pharmacol.* 394, 114961.
- Robertson, G.A., Morais-Cabral, J.H., 2020. hERG function in light of structure. *Biophys. J.* 118 (4), 790–797.
- Rohrbacher, J., Damiano, B.P., Girgis, I.G., Pugsley, M.K., Teisman, A., Gallacher, D.J., 2015. The source of hERG IC50 values (manual vs. automated patch clamp) may influence in silico modeling. *J. Pharmacol. Toxicol. Methods* 75, 167.
- Ryu, S., Imai, Y.N., Oiki, S., 2013. The synergic modeling for the binding of fluoroquinolone antibiotics to the hERG potassium channel. *Bioorg. Med. Chem. Lett.* 23 (13), 3848–3851.
- Shugg, T., Somberg, J.C., Molnar, J., Overholser, B.R., 2020. Inhibition of human ether-a-go-go-related gene (hERG) potassium current by the novel sotalol analogue, soestalol. *JACC Clin. Electrophysiol.* 6 (7), 756–759.
- Song, R., Wang, Y., Wang, M., Gao, R., Yang, T., Yang, S., Yang, C.-G., Jin, Y., Zou, S., Cai, J., Fan, R., He, Q., 2020. Design and synthesis of novel desfluoroquinolone-aminopyrimidine hybrids as potent anti-MRSA agents with low hERG activity. *Bioorg. Chem.* 103, 104176.
- Sridhar, A.R., Chatterjee, N.A., Saour, B., Nguyen, D., Starnes, E.A., Johnston, C., Green, M.L., Roth, G.A., Poole, J.E., 2020. QT interval and arrhythmic safety of hydroxychloroquine monotherapy in coronavirus disease 2019. *Heart Rhythm O2* 1 (3), 167–172.
- Stoelzle-Feix, S., Brinkwirth, N., Becker, N., Haarmann, C., Knox, R., Hampl, M., George, M., Vogel, M., Haedo, R., Fertig, N., 2020. Reliable identification of hERG liability in drug discovery by automated patch clamp. *J. Pharmacol. Toxicol. Methods* 105, 106743.
- Vandenberg, J.T., Perry, M.D., Perrin, M.J., Mann, S.A., Ke, Y., Hill, A.P., 2012. hERG K<sup>+</sup> channels: structure, function, and clinical significance. *Physiol. Rev.* 92 (3), 1393–1478.
- Vaz, R.J., Kang, J., Luo, Y., Rampe, D., 2018. Molecular determinants of loperamide and N-desmethyl loperamide binding in the hERG cardiac K<sup>+</sup> channel. *Bioorg. Med. Chem. Lett.* 28 (3), 446–451.
- Voisin, O., Lorc'h, E.L., Mahé, A., Azria, P., Borie, M.-F., Hubert, S., Ménage, E., Guillermin, J.-C., Mourad, J.-J., 2020. Acute QT interval modifications during hydroxychloroquine-azithromycin treatment in the context of COVID-19 infection. *Mayo Clin. Proc.* 95 (8), 1696–1700.
- Wang, W., MacKinnon, R., 2017. Cryo-EM structure of the open human Ether-à-go-go-related K<sup>+</sup> channel hERG. *Cell* 169 (3), 422–430.e410.
- Wu, W., Sanguinetti, M.C., 2016. Molecular basis of cardiac delayed rectifier potassium channel function and pharmacology. *Card. Electrophysiol. Clin.* 8 (2), 275–284.
- Zünkler, B.J., Wos, M., 2003. Effects of lomefloxacin and norfloxacin on pancreatic  $\beta$ -cell ATP-sensitive K<sup>+</sup> channels. *Life Sci.* 73 (4), 429–435.
- Zünkler, B.J., Claaßen, S., Wos-Maganga, M., Rustenbeck, I., Holzgrave, U., 2006. Effects of fluoroquinolones on HERG channels and on pancreatic  $\beta$ -cell ATP-sensitive K<sup>+</sup> channels. *Toxicology* 228 (2), 239–248.